High-Voltage Constraints for Vacuum Packaged Microstructures

Chester G. Wilson, *Member, IEEE*, Yogesh B. Gianchandani, *Member, IEEE*, and Amy E. Wendt

***Abstract*—In order to understand the details of high-field breakdown in microstructures that are vacuum packaged, a series of experiments are used to determine characteristics of microdischarges. The results support a reinterpretation of conventional assumptions based upon large scale discharges. When planar microelectrodes are used, Paschen's curve is not applicable in the traditional sense: the breakdown voltage is relatively insensitive to pressure in the 1–20 torr range, and remains at $\sim$400 V for air ambient. However, the spatial distribution of discharge current does vary with the pressure and the power. Large voltage gradients are supported in the glow region which is confined to a few millimeters directly above the cathode, and within a few hundred microns of its lateral edge. Their magnitudes range from 100 000–500 000 V/m for operating pressures ranging from 1.2–6 torr. Based on these results, guidelines are provided for the design of high-voltage microsystems. [916]**

***Index Terms*—Electric breakdown, electrostatic devices, microdischarge, microplasma.**

I. Introduction

ELECTROSTATIC sensing and actuation are pervasive in MEMS technology not only because of the wide variety of materials that they accommodate, but also because they are generally power efficient [1]–[4]. In many cases, performance measures such as sensitivity and dynamic range of sensors, or force and displacement of actuators are limited by the highest electric field that can be safely achieved, or voltage bias that can be applied. While there has been an incipient effort to study this phenomena at atmospheric pressure [5], most such devices are packaged in vacuum. In addition, the spatial distribution of the electric field and breakdown current, which are critical parameters for sustained avalanche breakdown, have not been reported in the context of microstructures. By addressing these questions, this paper attempts to establish design guidelines for high field devices.[1] . In doing so, it also addresses the requirements for sustained arcs and microplasmas which have been successfully used to etch silicon wafers and sense chemical impurities in liquids and gases [7], [8]. The experiments demonstrate that microdischarges violate many of the assumptions used routinely for larger scale discharges.

Manuscript received August 9, 2002; revised June 25, 2003. This work was supported in part by the National Science Foundation, U.S. Geological Survey, and the Sea Grant. Subject Editor T. Kenny.

C. G. Wilson and Y. B. Gianchandani are with the EECS Department, University of Michigan, Ann Arbor, MI 48109 USA (e-mail: yogesh@umich.edu).

A. E. Wendt is with the Department of Electrical and Computer Engineering, University of Wisconsin, Madison, WI 53706 USA.

Digital Object Identifier 10.1109/JMEMS.2003.820278

[1]Portions of this paper have appeared in conference abstract form in [6]

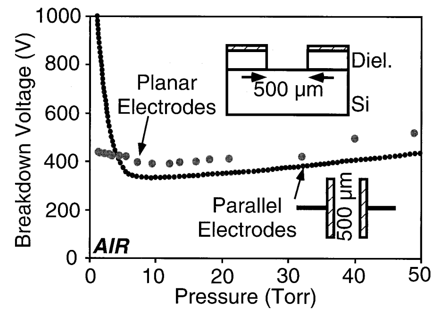

Fig. 1. Paschen voltage breakdown curve for parallel and planar electrodes with 500 μm spacing.

II. Structure and Experiment

For an electric discharge in a vacuum, breakdown voltage (BV) is believed to typically follow the Paschen curve [9], which indicates that a minimum BV is achieved at a particular product of pressure and separation between biased electrodes $(P \bullet d)$. At lower pressures, there are fewer collisions between molecules to trigger the avalanche process required for breakdown, while at higher pressures the mean free path (m.f.p.) of molecules is smaller, which reduces the velocity and energy of molecules at collision. Both of these effects necessitate a higher electric field to sustain the avalanche breakdown. However, with most microstructures, multiple path lengths are simultaneously available, which makes the discharge gap a variable, and permits a low BV to be sustained even as the pressure changes from the value that favors the minimum electrode separation. Fig. 1 illustrates the conventional Paschen curve for parallel plate electrodes, and measured voltage breakdown for planar electrodes spaced 500 μm apart at their nearest edges.

In order to measure the spatial distribution of discharge current, a sustained microdischarge was created between planar thin-film Ti electrodes on a glass substrate at vacuum levels ranging from 1 to 20 torr (see Fig. 2). Experiments were performed to measure the variation in the trajectory and current distribution of the positive ions and electrons. A segmented electrode 1 mm wide, 5 mm long, and spaced 0.4 mm apart was used first as an anode, and then as a cathode to measure these characteristics, which are dependent on both pressure and bias. The data presented is for a nitrogen ambient.

While undergoing the process of electrostatic breakdown, the voltage and current profiles of a microdischarge will vary. However, the discharge reaches a steady state in fractions of a microsecond [9]. After ignition, microdischarges in this pressure regime maintain a stable voltage and current. For all data presented in this work, the voltage and the current varied by no

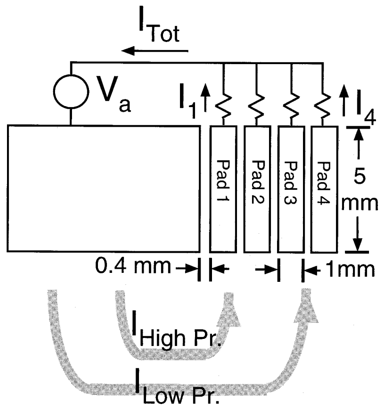

Fig. 2. Planar Ti electrode configuration, patterned on glass to measure cathode current density. Cathode is split into separate paths, where the current is independently measured. Polarity can be reversed to measure anode current density.

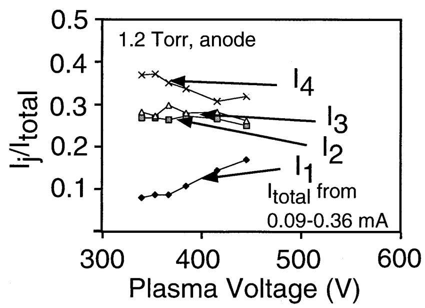

(a)

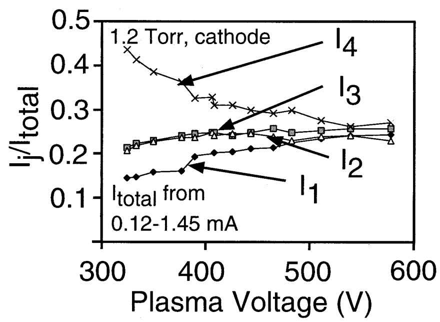

(b)

Fig. 3. Current reconstruction at 1.2 torr in N_2 for the (a) anode and (b) cathode.

more than 3% over a 15-min period, the stability of microdischarges is a large factor in the consistent silicon etch rates observed in prior work [7].

Fig. 3 shows that the cathode current favors longer paths at 1.2 torr. At low power and bias levels, the largest fraction of current was sustained by pad 4, the most distant, which was separated from the cathode by 4.6 mm. This fraction reduced as the power was increased, varying from about 40% to about 25%. This spread in current with increase in current density is consistent with expectation. Furthermore, at 6 torr the distribution in cathode current between the four pads was comparable (Fig. 4). In contrast, the same change in pressure resulted in a more dramatic change in the spatial distribution of anodic current: the fractional current in pad 4 changed from 37% at 1.2 torr to 7% at 6 torr.

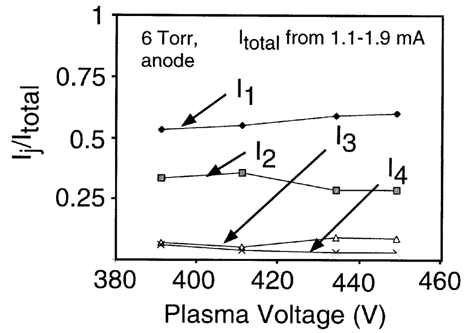

(a)

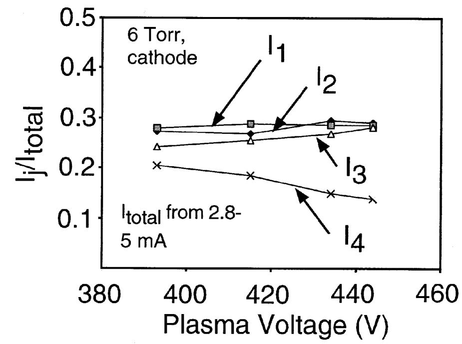

(b)

Fig. 4. Current reconstruction at 6 torr in N_2 for the (a) anode and (b) cathode.

The measurements can be explained as follows. In electric discharges, electrons are the dominant source of electrical current. Electron current is most prone to follow the path defined by the Paschen breakdown which requires the lowest energy. The $(P \bullet d)$ that provides the lowest breakdown voltage for N_2 is approximately 4 torr-mm [9]. This provides an approximate electron current path of 3.3 mm and 0.66 mm for 1.2 and 6 torr, respectively, which closely matches the experimentally determined paths of high-current density. A principal reason for the differences in the spatial distribution of current at the anode and cathode is related to the interaction cross section of the charged particle species. The m.f.p. of a $N_2 - N_2$ molecular collision at 1 torr is 51 μm. The electron-N_2 collisional m.f.p. is approximately 500 μm, varying by a factor of unity to approximately 50% with electron energy. The ion-N_2 m.f.p. is approximately 18 μm, and a function of ion energy [10]. Neutral molecules collide together, transferring energy and momentum in classical "billiard ball" collisions. Charged particles transfer energy to neutral atoms through electronic interaction; the electric field from the moving charged particle is seen as a time varying "pulse" by the neutral. This results in elastic scattering of the electron, or excitation and ionization of the neutral. The cross-sections of these electronic collisions are smaller than neutral-neutral collisions, and a function of the electric field pulse that is seen, hence the longer, energy dependent m.f.p.

Ions have a smaller m.f.p. than the molecule itself, as they can interact by collision *and* charge exchange mechanisms. In fact, the cross section for an interaction where a mobile ion receives an electron from a stationary neutral (creating a mobile neutral and a stationary ion) is larger than the "billiard ball" collision cross section [11]. Larger interaction cross sections result in smaller m.f.p.'s, and therefore, smaller particle mobilities. As

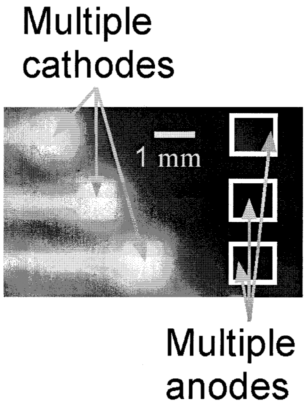

Fig. 5. Air microdischarges with varying electrode spacing show that the glow exists only over the cathode, and is independent of spacing, but dependent upon pressure and power density.

the electron m.f.p. is *longer* and the ion m.f.p is *shorter* than the neutrals, electron mobility is much greater than ion mobility. The difference in effective mobilities between ions and electrons results in the electron current being a stronger function of the electrode geometries. A portion of the cathode current is also formed by secondary electrons which are emitted where the ions strike the cathode. The spatial distribution of the secondary electrons are, therefore, largely governed by the trajectory of the heavier ions. Secondary electrons have a significant role in dc microdischarges as explained below.

One important aspect of microdischarges that differs from conventional discharges is that the glow is confined to the proximity of the cathode. Fig. 5 is an image of microdischarges generated on several anode–cathode combinations, with various electrode spacings. It is evident that under these conditions the confinement of the glow of the cathodes is not dependent on the anode-cathode spacing. Rather, it depends only on the ambient pressure and the microdischarge power density. As the ambient pressure increases, the glow region becomes better confined; as the power density increases, the glow becomes less confined. The localization of the glow over the cathode suggests that the ionization events in such microdischarges are largely dependent upon secondary electrons, which are emitted by the cathodes and are accelerated by the electric field into the region above. In contrast, larger scale plasmas have a glow region that extends between the electrodes, with a prominent dark sheath near the cathode. This phenomenon can be critical to the design of microdischarge-based sensors and display devices that have recently been reported [12]–[14].

Measurements of the potential distribution in microdischarges were performed using the arrangement shown in Fig. 6(a). A microdischarge was generated between the anode- cathode pair, which was formed by Ti patterned on a #7740 Corning glass wafer [see Fig. 6(b)]. The electrodes were 2 mm × 2 mm, with a 1 mm electrode spacing. The discharge was driven by a dc voltage source, V_a. The voltage probe was inserted into the region above the anode and the cathode, and was scanned vertically and horizontally. At each point the local floating potential, V_P was found by varying V_P' until the current through the resistor, which is proportional to the voltage V_2, is reduced to zero.

Fig. 7(a) and (b) show contour plots for the floating potential profiles for microdischarges generated at 2 torr and at 4

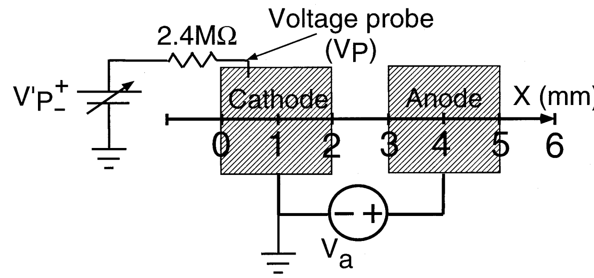

Fig. 6. Plasma floating potential V_P, is measured by varying applied voltage V_P' to find the value at which V_2 is zero. The planar electrodes are 2 mm × 2 mm.

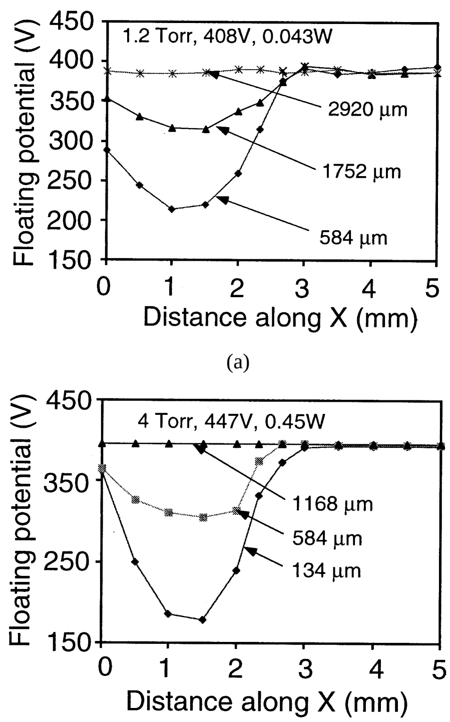

(a)

(b)

Fig. 7. Contour plots for floating potential as 1.2 torr (a) and 4 torr (b). Profiles are generated by the electrodes shown in Fig. 6. Voltage is measured along the X axis for varying heights over the coplanar electrodes. The plasma becomes more confined at higher pressures.

torr, respectively. The figures map the V_P in the space above the two electrodes. Three distinguishing observations of microdischarges can be made on the basis of these results. First, there is no discernable voltage drop over the anode, the only significant electric fields exist directly over the cathode. Second, there is a considerable voltage gradient in the glow region of microdischarges. This is in contrast to large scale plasmas, which do not have a significant voltage drop in the glow region. Finally, the extent of the glow, and the magnitude of the voltage drop are a function of the operating pressure. As the pressure is increased, the voltage gradient increases. Voltage gradients range from 100 000–500 000 V/m corresponding to 1.2–6 torr pressure. In contrast, traditional plasma discharges will typically support a 10–100 V/m voltage drop in the glow region. This provides further support for the proposition that ionization in microdischarges are created by the secondary electrons from the cathode being driven by the local electric field in the glow region.

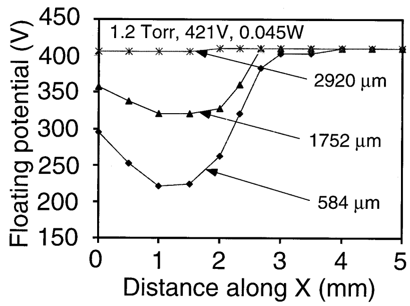

Fig. 8. Floating potential profile generated at 1.2 torr, with similar power density and electrode configuration to that shown in Fig. 6, except that electrode spacing is 4 mm, i.e., four times greater.

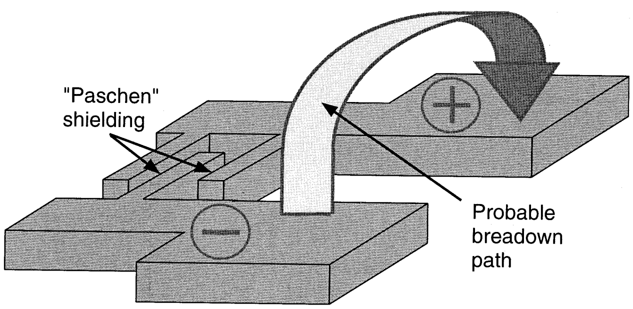

Fig. 9. Devices can be sized to increase breakdown voltage, or direct the breakdown to a less critical area.

In order to demonstrate the insensitivity of the field and glow region to electrode separation, an arrangement identical to that in Fig. 6(b), except that the electrode spacing was quadrupled to 4 mm, was used to generate a microdischarge at the same pressure and power density. The resulting floating potential profile, shown in Fig. 8, is essentially identical to Fig. 7(a).

III. Actuator Design Guidelines

It has been shown that there are considerable differences between microdischarges generated between planar electrodes in the 1–20 torr regime and traditional plasmas. The planar electrodes provide a more uniform breakdown voltage over a wide range of pressures than the traditional Paschen curve. The dimensions of the optimum electrode spacing for Paschen breakdown also correspond to the point of maximum current density after breakdown, over a wide range of vacuum levels. As a consequence, for vacuum packaged devices, the overall spacing on a device such as an electrostatic actuator is perhaps even more critical than the smallest distance between fingers, which was evaluated in [5]. As a consequence, for vacuum packaged actuators with dimensions of 5–10 mm, there will be a maximum voltage that is relatively independent of vacuum level. For the case of Ti electrodes in air the breakdown voltage is about 400 V. For smaller size or higher vacuum devices, the $(P \bullet d)$ that provides the lowest breakdown voltage, and highest current density for N_2 is approximately 4 torr-mm. This can be utilized to size the device during layout, or to design the device so breakdown occurs in a less critical area (see Fig. 9). Microdischarges are generated from secondary electron emission from the cathode, so breakdown voltage can be increased by insulation of the cathode only, or by using materials with low secondary electron emission coefficients.

IV. Conclusion

In conclusion, these results demonstrate how breakdown in vacuum varies with design parameters and operating conditions, and that it can be substantially different from conventional assumptions. For microdischarges generated on planar electrodes, electric breakdown does not follow the Paschen curve, there is a lower than expected breakdown voltage at small dimensions. Most of the glow in microdischarges is confined directly over the cathode. This glow region supports a strong voltage gradient, which is in contrast to traditional plasmas. It is likely that electric field driven secondary emission electrons produce the bulk of the ionization in microdischarges.

References

[1] L. J. Hornbeck, "Current status of the digital micromirror device (DMD) for projection television applications," in *Tech. Dig. IEEE Int. Electron Devices Meeting*, 1993, pp. 381–4.

[2] B. Gogoi, C. Chuan, and C. Mastrangelo, "Force balanced micro-machined pressure sensors," *IEEE Trans. Electron Devices*, vol. 48, pp. 1575–84, Aug. 2001.

[3] T. Tsuchiya, Y. Kageyama, H. Funabashi, and J. Sakata, "Polysilicon vibrating gyroscope vacuum encapsulated in an on-chip microchamber," *Sens. Actuators*, vol. A90, no. 1-2, pp. 49–55, May 2001.

[4] F. Ayazi, H. H. Chen, F. Kocer, H. Guong, and K. Najafi, "A HARPSS polysilicon vibrating ring gyroscope," *J. Microelectromech. Syst.*, vol. 10, pp. 169–79, June 2001.

[5] T. Ono, Y. Dong, and M. Esashi, "Microdischarge and electric breakdown in a micro-gap," *J. Micromech. Microeng.*, vol. 10, no. 3, pp. 445–51, Sept. 2000.

[6] C. G. Wilson, A. E. Wendt, and Y. B. Gianchandani, "High voltage limits for electrostatic transducers: On the role of ambient pressure and device dimension in microdischarges," in *Tech. Dig., Solid-State Sensor, Actuator, and Microsystems Workshop*, Hilton Head Island, SC, June 2002, pp. 370–1.

[7] C. Wilson and Y. Gianchandani, "Silicon micro-machining using in-situ DC microplasmas," *J. Microelectromech. Syst.*, vol. 10, pp. 50–4, Mar. 2000.

[8] J. C. T. Eijkel, H. Stoeri, and A. Manz, "A dc microplasma on a chip employed as an optical emission detector for gas chromatography," *Anal. Chem.*, vol. 72, pp. 2547–2552, June 2000.

[9] J. D. Cobine, *Gaseous Conduct.*, NY: Dover, 1958, pp. 17–18.

[10] L. G. H. Huxley and R. W. Crompton, *The Diffusion and Drift of Electrons in Gases*. New York: Wiley, 1974, pp. 627–631.

[11] M. A. Lieberman and A. J. Lichtenberg, *Principles of Plasma Discharges and Materials Processing*. New York: Wiley, 1994, pp. 64–77.

[12] C. G. Wilson and Y. B. Gianchandani, "Spectral detection of metal contaminants in water using an on-chip microglow discharge," *IEEE Trans. Electron Devices*, vol. 49, pp. 2317–2322, Dec. 2002.

[13] G. Jenkins and A. Manz, "Optical emission detection of liquid analytes using a micro-machined D.C. glow discharge device at atmospheric pressure," in *Proc. Micro Total Analysis Systems*, 2001, pp. 349–350.

[14] S. J. Park, J. Chen, C. Liu, and J. G. Eden, "Silicon microdischarge devices having inverted pyramidal cathodes: Fabrication and performance of arrays," *Appl. Phys. Lett.*, vol. 4, no. 78, pp. 419–21, Jan. 2001.

Chester G. Wilson (M'02) received the B.S. degree in electrical engineering in 1993, the M.S. degree in applied physics from the University of Washington in 1996, and the Ph.D. degree in electrical engineering from the University of Wisconsin-Madison in 2003.

He is currently working under Prof. Gianchandani, as a Research Fellow at the University of Michigan-Ann Arbor. He has also worked as an Adjuct Lecturer at the University of Michigan-Ann Arbor. He has studied topics in plasmas and microfabrication, and is currently focused on small scale discharge spectroscopic devices, the physics of microplasmas, and radiation detectors.

Dr. Wilson received the 2000–2001 Intel Foundation Fellowship Award and the 2002 University of Wisconsin Holbridge student paper award for his research in microplasmas.

Yogesh B. Gianchandani (S'83–M'85) received the B.S., M.S, and Ph.D. degrees in electrical engineering in 1984, 1986, and 1994, respectively.

He is presently with the Electrical Engineering and Computer Science Department at the University of Michigan, Ann Arbor. Prior to this, he was with the Electrical and Computer Engineering Department at the University of Wisconsin, Madison. He has also held industry positions with Xerox Corporation, Microchip Technology, and other companies, working in the area of integrated circuit design. His research interests include all aspects of design, fabrication, and packaging of micromachined sensors and actuators and their interface circuits.

Prof. Gianchandani serves on the Editorial Boards of Sensors and Actuators, IOP *Journal of Micromechanics and Microengineering*, and *Journal of Semiconductor Technology and Science*. He also served on the steering and technical program committees for the IEEE International Conference on Micro Electro Mechanical Systems (MEMS), and served as a General Co-Chair for this meeting in 2002.

Amy E. Wendt received the B.S. degree in engineering and applied science at California Institute of Technology (Caltech), Pasadena, in 1982 and the M.S. and Ph.D. degrees in electrical engineering and computer science at University of California at Berkeley in 1985 and 1988, respectively.

She is presently a Professor in the Department of Electrical and Computer Engineering at the University of Wisconsin-Madison. Her research encompasses diagnostics, modeling and design of plasma discharges for deposition, etching and modification of materials. She is currently the Group Leader for Plasma Etching in the University of Wisconsin-Madison Center for Plasma-Aided Manufacturing, and has served on the Executive Committee of the American Vacuum Society (AVS) Division of Plasma Science and Technology and has been the Program Committee of the annual AVS International Symposium since 1995.